Inorganic Chemistry
Article

Inorg. Chem. **2010**, *49*, 1551–1560 **1551**
DOI: 10.1021/ic901798y

Diverse Manganese(II) Coordination Polymers with Mixed Azide and Zwitterionic Dicarboxylate Ligands: Structure and Magnetic Properties

Yan-Qin Wang, Qin-Xiang Jia, Kun Wang, Ai-Ling Cheng, and En-Qing Gao*

Shanghai Key Laboratory of Green Chemistry and Chemical Processes, Department of Chemistry, East China Normal University, Shanghai 200062, China

Received September 9, 2009

The reactions of manganese(II) acetate or perchlorate, sodium azide, and the inner-salt-type dicarboxylate ligand 1,3-bis(4-carboxylato-1-pyridinium)propane (L) under different conditions yielded four different Mn^{II} coordination polymers with mixed azide and carboxylate bridges: $\{[Mn(L)(N_3)]ClO_4 \cdot 0.5H_2O\}_n$ (**1**), $\{[Mn_2(L)_2(N_3)_2][Mn(N_3)_4(H_2O)_2] \cdot 2H_2O\}_n$ (**2**), $\{[Mn_2(L)_2(N_3)_2(H_2O)_2]Br(N_3) \cdot 2H_2O\}_n$ (**3**), and $[Mn_4(L)_2(N_3)_8]_n$ (**4**). The compounds exhibit great diversity in their structures and magnetic properties. Both **1** and **2** contain anionic chains featuring a mixed $(OCO)_2(EO\text{-}N_3)$ triple bridge (EO = end-on) between adjacent Mn^{II} ions. In **1**, two independent sets of triple bridges with apparently different structural parameters alternate in the AABB sequence, and the resulting alternating chains are cross-linked into a cationic 3D framework by the cationic dipyridinium spacers. Differently, the chains in **2** have uniform bridges and are interlinked into a 2D coordination layer. An expression of the magnetic susceptibility for 1D systems with alternating $J_1J_1J_2J_2$ interactions has been deduced and applied to **1**. Magnetic studies on **1** and **2** reveal that the $(OCO)_2(EO\text{-}N_3)$ triple bridges induce antiferromagnetic coupling between Mn^{II} ions, and magnetostructural analyses suggest that the magnitude of the coupling can be correlated to the Mn−N and Mn−N−Mn parameters. Compound **3** contains 2D coordination layers in which the chains with alternating double EO-azide and double carboxylate bridges are interlinked by the dipyridinium spacers, and magnetic studies suggest alternating ferro- and antiferromagnetic interactions through the alternating bridges. The 3D framework of compound **4** is formed by the organic ligands interlinking the unique manganese−azide−carboxylate layers in which the $[Mn_4(\mu_3\text{-}N_3)_2(\mu_2\text{-}N_3)_2(\mu_2\text{-}COO)_4]$ clusters are interlinked through EE-azide bridges (EE = end-to-end). The structure represents a novel type of self-catenated 8-connected 3D net. Magnetostructural analyses suggest that all of the short bridging moieties in **4**, including $(\mu_3\text{-}EO\text{-}N_3)_2$, $(OCO)(EO\text{-}N_3)$, $(OCO)(EO\text{-}N_3)_2$, and single $EE\text{-}N_3$, propagate antiferromagnetic coupling.

Introduction

Recent years have witnessed great interest in the field of molecular magnetism, focusing on the understanding of magnetostructural correlations and the design of magnetic materials with potential applications.[1−3] The basic strategy to design such materials is to organize paramagnetic centers into polynuclear aggregates or polymeric networks by use of bridging ligands that can efficiently propagate magnetic superexchange. As a short bridging ligand and efficient superexchange mediator, the pesudohalide azido ion has proved to be very versatile and diverse in both coordination chemistry and magnetism.[4,5] Many azide-bridged systems with different dimensionality and topology have been synthesized by using various auxiliary ligands, and a great diversity of magnetic behaviors have been demonstrated.[4−9] A useful synthetic approach to obtaining new structures and magnetic

*To whom correspondence should be addressed. E-mail: eqgao@chem.ecnu.edu.cn. Fax: +86-21-62233404.

(1) (a) Gatteschi, D.; Kahn, O.; Miller, J.-S.; Palacio, F. *Magnetic Molecular Materials*; Kluwer Academic: Dordrecht, The Netherlands, 1991. (b) Kahn, O. *Molecular Magnetism*; VCH: New York, 1993.

(2) (a) Miller, J.-S.; Epstein, A.-J. *Angew. Chem., Int. Ed. Engl.* **1994**, *33*, 385. (b) Miller, J.-S.; Epstein, A.-J. *Angew. Chem.* **1994**, *106*, 399. (c) *Molecular Magnetism: from Molecular Assemblies to Devices*; Coronado, E., Delhaes, P., Gatteschi, D., Miller, J.-S., Eds.; NATO ASI Series 15; Kluwer: Dordrecht, The Netherlands, 1995; Vol. *321*.

(3) (a) Miller, J.-S. *Adv. Mater.* **2002**, *14*, 1105. (b) *Magnetism: Molecules to Materials*; Miller, J.-S., Drilon, M., Eds.; Wiley-VCH: Weinheim, Germany, 2002−2005; Vol. *I*−*V*. (c) Gatteschi, D.; Sessoli, R. *Angew. Chem., Int. Ed.* **2003**, *42*, 268.

(4) (a) Ribas, J.; Escuer, A.; Monfort, M.; Vicente, R.; Cortés, R.; Lezama, L.; Rojo, T. *Coord. Chem. Rev.* **1999**, *193*, 1027. (b) Wang, X.-Y.; Wang, Z.-M.; Gao, S. *Chem. Commun.* **2008**, *3*, 281. (c) Zeng, Y.-F.; Hu, X.; Liu, F.-C.; Bu, X.-H. *Chem. Soc. Rev.* **2009**, *38*, 469. (d) Escuer, A.; Aromí, G. *Eur. J. Inorg. Chem.* **2006**, *23*, 4721.

(5) (a) Gao, E.-Q.; Liu, P.-P.; Wang, Y.-Q.; Yue, Q.; Wang, Q.-L. *Chem.—Eur. J.* **2009**, *15*, 1217. (b) Sun, H.-L.; Gao, S.; Ma, B.-Q.; Su, G.; Batten, S.-R. *Cryst. Growth Des.* **2005**, *5*, 269. (c) Gao, E.-Q.; Wang, Z.-M.; Yan, C.-H. *Chem. Commun.* **2003**, 1748.

(6) (a) Yang, C.-I.; Wernsdorfer, W.; Lee, G.-H.; Tsai, H.-L. *J. Am. Chem. Soc.* **2007**, *129*, 456. (b) Stamatatos, T.-C.; Abboud, K.-A.; Wernsdorfer, W.; Christou, G. *Angew. Chem., Int. Ed.* **2007**, *46*, 844. (c) Boudalis, A.-K.; Pissas, M.; Raptopoulou, C.-P.; Psycharis, V.; Abarca, B.; Ballesteros, R. *Inorg. Chem.* **2008**, *47*, 10674. (d) Stamatatos, T.-C.; Abboud, K. A.; Wernsdorfer, W.; Christou, G. *Angew. Chem., Int. Ed.* **2008**, *47*, 6694.

Published on Web 01/22/2010

properties is to incorporate a second short bridge that provides different pathways for magnetic exchange. Considering that the carboxylate group can also efficiently transmit superexchange,[10−16] we are interested in combining azide and carboxylate into one system. More interestingly, the combination of azide and dicarboxylate ligands may lead to high-dimensional networks, providing an opportunity to tune the structure and magnetism by changing the organic spacer between carboxylate groups. However, only a limited number of systems with azide and carboxylate simultaneously bridging neighboring metal ions have been reported, where the carboxylate bridges mainly come from simple monocarboxylates (formate or acetate)[17,18] or pyridylcarboxylate-derived ligands.[19,20] The approach using the usual dicarboxylates as coligands in metal azide systems seldom succeeded in giving the expected materials with simultaneous azide and carboxylate bridges.[21] The difficulty may arise from the unbalanced competition of the two anionic bridges in binding metal ions and compensating for the metal charge. To overcome this, we proposed employing the inner-salt-type (or zwitterionic) ligands bearing separated positive (pyridinium) and negative (carboxylate) charges, as exemplified in Chart 1. Such dicarboxylate ligands are overall neutral, and thus the simultaneous coordination of azide and carboxylate is facilitated, giving high-dimensional networks with various magnetic properties, as we have demonstrated recently.[22]

Chart 1

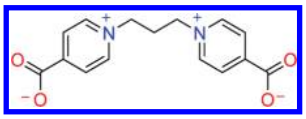

Here we report the structures and magnetic properties of four different coordination polymers obtained from the reactions of manganese(II) salts and azide in the presence of the neutral dicarboxylate ligand 1,3-bis(4-carboxylato-1-pyridinium)propane (L, Chart 1). Their formulas are $\{[Mn(L)(N_3)]ClO_4\cdot 0.5\,H_2O\}_n$ (**1**), $\{[Mn_2(L)_2(N_3)_2][Mn(N_3)_4(H_2O)_2]\cdot 2H_2O\}_n$ (**2**), $\{[Mn_2(L)_2(N_3)_2(H_2O)_2]Br(N_3)\cdot 2H_2O\}_n$ (**3**), and $[Mn_4(L)_2(N_3)_8]_n$ (**4**). The charge balance in these compounds is achieved in different ways, depending upon the reaction conditions, and the azide and carboxylate bridges are mixed in different fashions to give different bridging networks, including alternating (**1**) or uniform (**2**) chains with $(OCO)_2(N_3)$ triple bridges, chains with alternating $(OCO)_2$ and $(N_3)_2$ bridges (**3**), and Mn_4-cluster-based layers containing four different bridging moieties (**4**). The different magnetic behaviors for these diverse structures are revealed and analyzed, and some magnetostructural correlations have been proposed. Compound **4** has been preliminarily communicated elsewhere.[22a]

Experimental Section

Materials and Physical Measurements. Elemental analyses were determined on an Elementar Vario ELIII analyzer. The FT-IR spectra were recorded in the range 500−4000 cm^{-1} using KBr pellets on a Nicolet NEXUS 670 spectrophotometer. The phase purity of the bulk or polycrystalline samples was verified by powder X-ray diffraction (PXRD) measurements performed on a Bruker D8-Advance diffractometer equipped with Cu Kα at a scan speed of 1° min^{-1}. The measured patterns are consistent with those calculated from the crystal data (see the Supporting Information). Temperature-dependent magnetic measurements were performed on a Quantum Design MPMS-XL5 SQUID magnetometer. The experimental susceptibilities

(7) (a) Stamatatos, T. C.; Abboud, K. A.; Wernsdorfer, W.; Christou, G. *Inorg. Chem.* **2009**, *48*, 807. (b) Massoud, A. A.; Abu-Youssef, M. A. M.; Vejpravova, J. P.; Langera, V.; Ohrstrom, L. *CrystEngComm* **2009**, *11*, 223.
(8) (a) Liu, P.-P.; Cheng, A.-L.; Liu, N.; Sun, W.-W.; Gao, E.-Q. *Chem. Mater.* **2007**, *19*, 2724. (b) Abu-Youssef, M. A. M.; Escuer, A.; Mautner, F. A.; Öhrström, L. *Dalton Trans.* **2008**, 3553. (c) Gao, E.-Q.; Yue, Y.-F.; Bai, S.-Q.; He, Z.; Yan, C.-H. *J. Am. Chem. Soc.* **2004**, *126*, 1419. (d) Escuer, A.; Mautner, F. A.; Goher, M. A. S.; Abu-Youssef, M. A. M.; Vicente, R. *Chem. Commun.* **2005**, 605.
(9) (a) Gao, E.-Q.; Bai, S.-Q.; Yue, Y.-F.; Wang, Z.-M.; Yan, C.-H. *Inorg. Chem.* **2003**, *42*, 3642. (b) Gao, E.-Q.; Cheng, A.-L.; Xu, Y.-X.; He, M.-Y.; Yan, C.-H. *Inorg. Chem.* **2005**, *44*, 8822. (c) Yu, M.-M.; Ni, Z.-H.; Zhao, C.-C.; Cui, A.-L.; Kou, H.-Z. *Eur. J. Inorg. Chem.* **2007**, 5670. (d) Bai, S.-Q.; Gao, E.-Q.; He, Z.; Fang, C.-J.; Yue, Y.-F.; Yan, C.-H. *Eur. J. Inorg. Chem.* **2006**, 407.
(10) (a) Jia, H.-P.; Li, W.; Ju, Z.-F.; Zhang, J. *Dalton Trans.* **2007**, *33*, 3699. (b) Suárez-Varela, J.; Mota, A. J.; Aouryaghal, H.; Cano, J.; Rodríguez-Diéguez, A.; Luneau, D.; Colacio, E. *Inorg. Chem.* **2008**, *47*, 8143. (c) Yao, M.-X.; Zeng, M.-H.; Zou, H.-H.; Zhou, Y.-L.; Liang, H. *Dalton Trans.* **2008**, 2428. (d) Psomas, G.; Raptopoulou, C. P.; Iordanidis, L.; Dendrinou-Samara, C.; Tangoulis, V.; Kessissoglou, D. P. *Inorg. Chem.* **2000**, *39*, 3042.
(11) (a) Zhang, J.-Y.; Ma, Y.; Cheng, A.-L.; Yue, Q.; Sun, Q.; Gao, E.-Q. *Dalton Trans.* **2008**, 2061. (b) Baldomá, R.; Monfort, M.; Ribas, J.; Solans, X.; Maestro, M. A. **2006**, *45*, 8144. (c) Jia, L.-H.; Liu, Z.-L.; Zhu, L.; Liu, W.; Yao, K.-L. *J. Chem. Phys.* **2007**, *127*, 064702. (d) Zeng, M.-H.; Wu, M.-C.; Liang, H.; Zhou, Y.-L.; Chen, X.-M.; Ng, S.-W. *Inorg. Chem.* **2007**, *46*, 7241.
(12) (a) Li, W.; Jia, H.-P.; Ju, Z.-F.; Zhang, J. *Dalton Trans.* **2008**, 5350. (b) Durot, S.; Policar, C.; Pelosi, G.; Bisceglie, F.; Mallah, T.; Mahy, J.-P. *Inorg. Chem.* **2003**, *42*, 8072. (c) Chen, X.-M.; Tong, Y.-X.; Xu, Z.-T.; Mak, T. C. W. *J. Chem. Soc., Dalton Trans.* **1995**, 4001. (d) Policar, C.; Lambert, F.; Cesario, M.; Morgenstern-Badarau, I. *Eur. J. Inorg. Chem.* **1999**, 2201.
(13) (a) Liu, C.-M.; Zhang, D.-Q.; Zhu, D.-B. *Inorg. Chem.* **2009**, *48*, 4980. (b) Tangoulis, V.; Psomas, G.; Dendrinou-Samara, C.; Raptopoulou, C. P.; Terzis, A.; Kessissoglou, D. P. *Inorg. Chem.* **1996**, *35*, 7655. (c) Maji, T. K.; Sain, S.; Mostafa, G.; Lu, T.-H.; Ribas, J.; Monfort, M.; Chaudhuri, N. R. *Inorg. Chem.* **2003**, *42*, 709. (d) Chiang, W.; Ho, D. M.; Engen, D. V.; Thompson, M. E. *Inorg. Chem.* **1993**, *32*, 2886.
(14) (a) Wang, R.-H.; Yuan, D.-Q.; Jiang, F.-L.; Han, L.; Gao, S.; Hong, M.-C. *Eur. J. Inorg. Chem.* **2006**, 1649. (b) Albela, B.; Corbella, M.; Ribas, J.; Castro, I.; Sletten, J.; Stoeckli-Evans, H. *Inorg. Chem.* **1998**, *37*, 788. (c) Chen, W.; Yue, Q.; Chen, C.; Yuan, H.-M.; Xu, W.; Chen, J.-S.; Wang, S.-N. *Dalton Trans.* **2003**, 28. (d) Rardin, R. L.; Tolman, W. B.; Lippard, S. J. *New J. Chem.* **1991**, *15*, 417.
(15) (a) Oshio, H.; Ino, E.; Magi, I.; Ito, T. *Inorg. Chem.* **1993**, *32*, 5697. (b) Konar, S.; Manna, S. C.; Zangrando, E.; Mallah, T.; Ribas, J.; Chaudhuri, N. R. *Eur. J. Inorg. Chem.* **2004**, 4202. (c) Fernández, G.; Corbella, M.; Mahía, J.; Maestro, M. A. *Eur. J. Inorg. Chem.* **2002**, 2502.
(16) Lecren, L.; Roubeau, O.; Li, Y.-G.; Goff, X. F. L.; Miyasaka, H.; Richard, F.; Wernsdorfer, W.; Coulon, C.; Clérac, R. *Dalton Trans.* **2008**, 755.
(17) (a) Thompson, L. K.; Tandon, S. S.; Lloret, F.; Cano, J.; Julve, M. *Inorg. Chem.* **1997**, *36*, 3301. (b) Liu, T.; Zhang, Y.-J.; Wang, Z.-M.; Gao, S. *Inorg. Chem.* **2006**, *45*, 2782. (c) Wang, X.-T.; Wang, X.-H.; Wang, Z.-M.; Gao, S. *Inorg. Chem.* **2009**, *48*, 1301.
(18) (a) Milios, C. J.; Prescimone, A.; Sanchez-Benitez, J.; Parsons, S.; Murrie, M.; Brechin, E. K. *Inorg. Chem.* **2006**, *45*, 7053. (b) Demeshko, S.; Leibeling, G.; Maringgele, W.; Meyer, F.; Mennerich, C.; Klauss, H.-H.; Pritzkow, H. *Inorg. Chem.* **2005**, *44*, 519. (c) Mondal, K. C.; Sengupta, O.; Nethaji, M.; Mukherjee, P. S. *Dalton Trans.* **2008**, *6*, 767.
(19) (a) He, Z.; Wang, Z.-M.; Gao, S.; Yan, C.-H. *Inorg. Chem.* **2006**, *45*, 6694. (b) Chen, H.-J.; Mao, Z.-W.; Gao, S.; Chen, X.-M. *Chem. Commun.* **2001**, 2320. (c) Liu, F.-C.; Zeng, Y.-F.; Li, J.-R.; Bu, X.-H.; Zhang, H.-J.; Ribas, J. *Inorg. Chem.* **2005**, *44*, 7298.
(20) (a) Liu, F.-C.; Zeng, Y.-F.; Jiao, J.; Bu, X.-H.; Ribas, J.; Batten, S. R. *Inorg. Chem.* **2006**, *45*, 2776. (b) Zeng, Y.-F.; Zhao, J.-P.; Hu, B.-W.; Hu, X.; Liu, F.-C.; Ribas, J.; Arino, J. R.; Bu, X.-H. *Chem.—Eur. J.* **2007**, *13*, 9924.
(21) (a) Escuer, A.; Vicente, R.; Mautner, F. A.; Goher, M. A. S. *Inorg. Chem.* **1997**, *36*, 1233. (b) Li, L. C.; Liao, D. Z.; Jiang, Z. H.; Yan, S. P. *Polyhedron* **2001**, *20*, 681. (c) Han, Y.-F.; Wang, T.-W.; Song, Y.; Shen, Z.; You, X.-Z. *Inorg. Chem. Commun.* **2008**, *11*, 207. (d) Hong, C. S.; You, Y. S. *Polyhedron* **2004**, *23*, 1379.
(22) (a) Wang, Y.-Q.; Zhang, J.-Y.; Jia, Q.-X.; Gao, E.-Q.; Liu, C.-M. *Inorg. Chem.* **2009**, *48*, 789. (b) Tian, C.-Y.; Sun, W.-W.; Jia, Q.-X.; Tian, H.; Gao, E.-Q. *Dalton Trans.* **2009**, 6109. (c) Ma, Y.; Zhang, J.-Y.; Cheng, A.-L.; Sun, Q.; Gao, E.-Q.; Liu, C.-M. *Inorg. Chem.* **2009**, *48*, 6142. (d) Sun, W.-W.; Tian, C.-Y.; Jing, X.-H.; Wang, Y.-Q.; Gao, E.-Q. *Chem. Commun.* **2009**, 4741.

Table 1. Crystal Data and Structure Refinement for Compounds **1**−**4**

	1	**2**	**3**	**4**
formula	$C_{15}H_{15}ClMnN_5O_{8.5}$	$C_{30}H_{36}Mn_3N_{22}O_{12}$	$Mn_2C_{30}H_{36}N_{13}O_{12}Br$	$C_{30}H_{28}Mn_4N_{28}O_8$
M_r	491.71	1061.63	960.51	1128.56
cryst syst	monoclinic	monoclinic	triclinic	orthorhombic
space group	$P2_1/c$	$C2/m$	$P\bar{1}$	$Pbca$
a [Å]	14.1561(17)	20.103(9)	7.49280(10)	13.7371(5)
b [Å]	10.5239(13)	7.623(3)	10.82610(10)	15.6580(5)
c [Å]	27.033(3)	13.549(6)	12.19460(10)	19.9617(7)
β [deg]	100.649(3)	97.323(7)	104.7710(10)	90
V [Å^3]	3958.0(8)	2059.3(16)	952.471(17)	4293.7(3)
Z	8	2	1	4
ρ_{calcd} [g cm^{-3}]	1.650	1.712	1.675	1.746
μ [mm^{-1}]	0.860	0.995	1.790	1.234
unique reflns	6918	2503	4405	4970
R_{int}	0.0619	0.0586	0.0207	0.0500
R1 [$I > 2\sigma(I)$]	0.1111	0.0651	0.0339	0.0337
wR2 (all data)	0.2874	0.1826	0.0976	0.0874

were corrected for the diamagnetism of the constituent atoms (Pascal's tables).

Synthesis. The reagents were obtained from commercial sources and used without further purification. 1,3-Bis(4-carboxylato-1-pyridinium)propane dihydrobromide ($[H_2L]Br_2$) was prepared according to the literature.[23]

Caution! *Although not encountered in our experiments, azido compounds of metal ions are potentially explosive. Only a small amount of the material should be prepared, and it should be handled with care.*

$\{[Mn(L)(N_3)]ClO_4\cdot 0.5H_2O\}_n$ (1). $[H_2L]Br_2$ (0.0448 g, 0.1 mmol) and sodium azide (0.026 g, 0.4 mmol) were dissolved into a mixture of ethanol (2 mL) and water (2 mL), and then the solution was added into an ethanol solution (2 mL) of $Mn(ClO_4)_2\cdot 6H_2O$ (0.0791 g, 0.2 mmol). The mixture was stirred for a few minutes, yielding a little orange-yellow precipitate, which was filtered off. Slow evaporation of the filtrate at room temperature afforded orange-yellow crystals of **1** after 1 day. The crystals were collected by filtration, washed by water and ethanol, and dried in air. Yield: 35.6% based on L. Mixing $Mn(ClO_4)_2$ and $[H_2L]Br_2$ in aqueous ethanol in a 1:1 ratio in the presence of excessive NaN_3 yielded a polycrystalline product of **1**, as confirmed by IR and PXRD measurements. Elem anal. Calcd for $C_{15}H_{15}ClMnN_5O_{8.5}$: C, 36.64; H, 3.07; N, 14.24. Found: C, 37.18; H, 3.43; N, 14.45. Main IR bands (KBr, cm^{-1}): 2082s [$\nu(N_3)$], 2062s [$\nu(N_3)$], 1613s [ν_{as}(COO)], 1568m, 1461m, 1396s [ν_s(COO)], 1379s, 1096s [$\nu(ClO_4)$], 784m, 694m.

$\{[Mn_2(L)_2(N_3)_2][Mn(N_3)_4(H_2O)_2]\cdot 2H_2O\}_n$ (2). A mixture solution of $Mn(OAc)_2\cdot 4H_2O$ (0.049 g, 0.2 mmol), NaN_3(0.065 g, 1.0 mmol), and $[H_2L]Br_2$ (0.0448 g, 0.1 mmol) in ethanol (4 mL) and water (1 mL) was sealed in a Teflon-lined stainless steel vessel (25 mL), heated at 70 °C for 4 days under autogenous pressure, and then cooled to room temperature. Yellow plate crystals of **2** were obtained in a yield of 85% based on L. Anal. Calcd for $Mn_3C_{30}H_{36}N_{22}O_{12}$: C, 33.94; H, 3.42; N, 29.03. Found: C, 34.41; H, 3.76; N, 29.37. Main IR bands (KBr, cm^{-1}): 2085s [$\nu(N_3)$], 2036s [$\nu(N_3)$], 1619s [ν_{as}(COO)], 1564s, 1465m, 1391s [ν_s(COO)], 1176m, 782m, 688m.

$\{[Mn_2(L)_2(N_3)_2(H_2O)_2]Br(N_3)\cdot 2H_2O\}_n$ (3). A mixture solution of $Mn(OAc)_2\cdot 4H_2O$ (0.049 g, 0.2 mmol), NaN_3(0.0195 g, 0.3 mmol), and $[H_2L]Br_2$ (0.0896 g, 0.2 mmol) in ethanol (4 mL) and water (1.5 mL) was sealed in a Teflon-lined stainless steel vessel (25 mL), heated at 70 °C for 4 days under autogenous pressure, and then cooled to room temperature. Orange block crystals of **3** were obtained in a yield of 40.5% based on L. Anal. Calcd for $Mn_2C_{30}H_{36}N_{13}O_{12}Br$: C, 37.52; H, 3.78; N, 18.96. Found: C, 37.28; H, 4.10; N, 18.58. Main IR bands (KBr, cm^{-1}): 2066s [$\nu(N_3)$], 2018s [$\nu(N_3)$], 1639s, 1620s [ν_{as}(COO)] 1567s, 1453m, 1386s [ν_s(COO)], 1179m, 783m, 690m.

$[Mn_4(L)_2(N_3)_8]_n$ (4). A mixture solution of $Mn(OAc)_2\cdot 4H_2O$ (0.049 g, 0.2 mmol), $[H_2L]Br_2$ (0.0448 g, 0.1 mmol), and NaN_3 (0.065 g, 1.0 mmol) in water (2 mL) and ethanol (4 mL) was allowed to stand at room temperature, and red crystals of **4** were obtained in 1 week. Yield: 27.5% based on L. Anal. Calcd for $C_{30}H_{28}Mn_4N_{28}O_8$: C, 31.91; H, 2.50; N, 34.72. Found: C, 31.94; H, 2.90; N, 34.50. Main IR bands (KBr, cm^{-1}): 2076s [$\nu(N_3)$], 2038s [$\nu(N_3)$], 1619s [ν_{as}(COO)], 1563m, 1450m, 1396s [ν_s(COO)], 1334w, 1309w, 780m, 690m.

X-ray Crystallography. Diffraction data for **1**−**4** were collected at room temperature on a Bruker Apex II CCD area detector equipped with graphite-monochromated Mo Kα radiation (λ = 0.710 73 Å). Empirical absorption corrections were applied using the *SADABS* program.[24] The structures were solved by direct methods and refined by the full-matrix least-squares method on F^2, with all non-hydrogen atoms refined with anisotropic thermal parameters.[25] All of the hydrogen atoms attached to carbon atoms were placed in calculated positions and refined using the riding model, and the water hydrogen atoms in **1**−**3** were located from difference maps. The octahedrally coordinated Mn2 site in **2** has a symmetry of 2/*m*, with the mirror passing the two axial azide ions and the 2-fold axis lying in the equatorial plane. This crystallographic symmetry is higher than the actual coordination symmetry, making the equatorial ligands (azide and water) disordered at two sets of symmetry-related sites around Mn2, with $^1/_2$ occupancy for each set (see the Supporting Information). The structure can also be solved in the lower-symmetry *C*2 and *Cm* space groups, but disorder of the Mn2 coordination environment remains. Efforts to avoid disorder by expanding the unit cell were in vain. A summary of the crystallographic data, data collection, and refinement parameters for complexes **1**−**4** is provided in Table 1.

Results and Discussion

Synthesis. The compounds were synthesized by the reactions of $Mn(ClO_4)_2$ or $Mn(OAc)_2$, NaN_3, and $[H_2L]Br_2$ in aqueous ethanol. Compounds **1** and **4** were obtained by allowing the solution containing the reactants to stand at room temperature. The use of $Mn(ClO_4)_2$ led to **1**, which contains perchlorate as lattice counteranions, while the use of $Mn(OAc)_2$ yielded **4**, which is free of lattice anions. Excessive NaN_3 has been used in the syntheses, which could act as a weak base to deprotonate $[H_2L]Br_2$ besides serving as the ligand to

(23) Mao, J.-G. *Chinese J. Struct. Chem.* **1998**, *17*(5), 353.

(24) Sheldrick, G. M. *Program for Empirical Absorption Correction of Area Detector Data*; University of Göttingen: Göttingen, Germany, 1996.

(25) Sheldrick, G. M. *SHELXTL*, version 5.1; Bruker Analytical X-ray Instruments Inc.: Madison, WI, 1998.

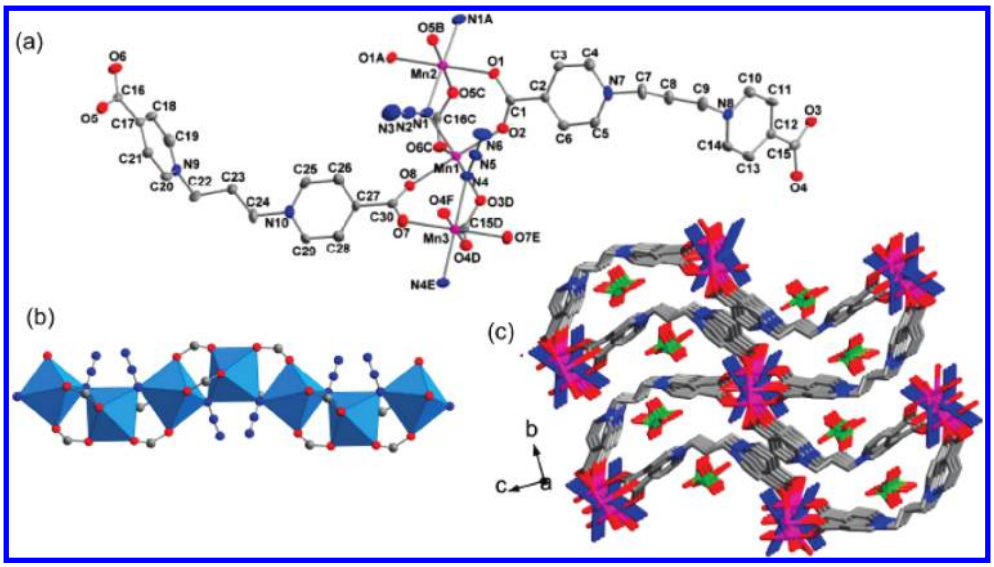

Figure 1. (a) Local coordination environments of the manganese centers and the ligands in compound **1**. Hydrogen atoms are omitted for clarity, and symmetry codes are (A) $1-x, 1-y, 1-z$, (B) $x, 0.5-y, z-0.5$, (C) $1-x, 0.5+y, 1.5-z$, (D) $x, 1.5-y, 0.5+z$, (E) $-x, 1-y, 1-z$, and (F) $-x, -0.5+y, 0.5-z$. (b) 1D chain along the *c* direction in compound **1**. (c) 3D network of **1**.

bind metal ions. Both compounds could be prepared using the stoichiometric M:L ratios of 1:1 and 2:1, respectively, although single crystals of **1** were grown in the presence of excessive $Mn(ClO_4)_2$. Compounds **2** and **3** were synthesized by heating the reaction mixtures in a sealed vessel at 70 °C. Compound **2** was obtained by using excessive manganese salt and sodium azide (the starting $M:L:N_3$ ratio is 2:1:10). When a stoichiometric $M:L:N_3$ ratio of 3:2:6 for **2** was used, the reaction yielded compound **3**, which has a stoichiometric $M:L:N_3$ ratio of 2:2:3. Compound **3** could also be prepared using the stoichiometric ratio $M:L:N_3 = 2:2:3$.

Description of the Structures. Compound 1. The compound exhibits a 3D anionic framework consisting of $[Mn(N_3)(COO)_2]_n$ chains connected by 1,3-bis(1-pyridinium)propane spacers. The coordination environments of the metal ions are shown in Figure 1a. There are three crystallographically independent Mn^{II} ions, each residing in the $[N_2O_4]$ environment completed by two azide ions and four carboxylate groups. For each manganese, the Mn−N distances [2.206(8)−2.242(8) Å] are longer than Mn−O [2.142(7)−2.206(6) Å]. While Mn2 and Mn3 are located at different inversion centers with the axially elongated trans-octahedral geometry, the Mn1 site is asymmetric with the cis-octahedral geometry (the two nitrogen atoms are at neighboring vertices of the octahedron). The metal ions alternate in the −Mn1−Mn2−Mn1−Mn3− repeating sequence, and the neighboring metal ions are triply bridged by two carboxylate groups in the syn−syn mode and an azide ligand in the end-on (EO) mode, generating an infinite chain along the *c* direction, in which metal octahedra share corners (the bridging azide nitrogen atoms; Figure 1b). The triple bridges between Mn1 and Mn2 and between Mn1 and Mn3 are somewhat different in structural parameters. The $Mn1(OCO)_2(N_3)Mn3$ moiety has longer Mn−N/O distances, a larger Mn−N−Mn angle, and, consistently, a longer Mn···Mn distance than $Mn1(OCO)_2(N_3)Mn2$, as shown in Table 2. The carboxylate bridges also show different degrees of distortion. Typically, the syn−syn bridging mode has bridged metal ions lying in or near the OCO plane, with zero or small M−O−C−O torsion angles. In **1**, the carboxylate bridging modes are significantly distorted toward the syn−anti mode, with the largest Mn−O−C−O torsion angles being 74.9° for the Mn1−Mn2 pair and 59.9° for Mn1−Mn3. The distortions lead to nonplanar but spiral conformations for the M−O−C−O−M moieties.

The L ligand in the structure serves as a μ_4 bridge, using its two carboxylate groups to bind two pairs of metal ions from two chains, and the trimethylene tether between the pyridinium rings adopts the trans−trans conformation to generate a bent shape for the ligand. Through the bent

Table 2. Selected Distances (Å) and Angles (deg) for the $(OCO)_2(N_3)$ Triple Bridges in **1** and **2**

For $Mn1(OCO)_2(N_3)Mn2$ in **1**			
Mn1−N1	2.208(8)	Mn2−N1	2.206(8)
Mn1−O2	2.157(7)	Mn2−O1	2.194(6)
Mn1−O6C	2.192(7)	Mn2−O5C	2.142(7)
Mn1···Mn2	3.641(2)	Mn1−N1−Mn2	111.1(4)
Mn1−O2−C1−O1	37.80(14)	Mn2−O1−C1−O2	6.90(15)
Mn1−O6C−C16C−O5C	27.01(13)	Mn2−O5C−C16C−O6C	74.86(12)
For $Mn1(OCO)_2(N_3)Mn3$ in **1**			
Mn1−O8	2.186(7)	Mn3−O4D	2.206(6)
Mn1−O3D	2.204(7)	Mn3−O7	2.184(7)
Mn1−N4	2.242(8)	Mn3−N4	2.222(8)
Mn1···Mn3	3.814(2)	Mn1−N4−Mn3	117.4(4)
Mn1−O8−C30−O7	25.35(19)	Mn3−O4D−C15D−O3D	59.93(14)
For $Mn1(OCO)_2(N_3)Mn1A$ in **2**			
Mn1−N3	2.234(3)	Mn1−O2B	2.170(3)
Mn1−O1	2.176(3)	Mn1−N3−Mn1A	117.0(2)
Mn1−O1−C1−O1A	28.95(74)	Mn1−O2B−C11C−O2C	37.45(73)
Mn1···Mn1A	3.811(2)		

Symmetry codes for **1**: (A) $1-x, 1-y, 1-z$; (B) $x, 0.5-y, z-0.5$; (C) $1-x, 0.5+y, 1.5-z$; (D) $x, 1.5-y, 0.5+z$. Symmetry codes for **2**: (A) $x, 1-y, z$; (B) $1-x, 1-y, 2-z$; (C) $1-x, y, 2-z$.

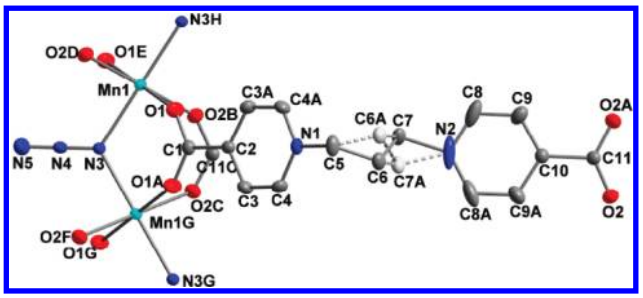

Figure 2. Local coordination environments of the manganese center and the ligands in compound **2**. Hydrogen atoms are omitted for clarity, and symmetry codes are (A) $x, 1-y, z$, (B) $1-x, 1-y, 2-z$, (C) $1-x, y, 2-z$, (D) $x-{}^1/_2, y-{}^1/_2, z-1$, (E) ${}^1/_2-x, {}^1/_2-y, 1-z$, (F) $x-{}^1/_2, {}^3/_2-y, z-1$, (G) ${}^1/_2-x, {}^1/_2+y, 1-z$, and (H) ${}^1/_2-x, y-{}^1/_2, 1-z$. The disorder of the methylene groups in the ligand is also shown.

ligands in four different directions, each $[Mn(N_3)(COO)_2]_n$ chain is linked to four identical chains, producing a 3D framework (Figure 1c). The shortest interchain Mn···Mn distance is about 10.0 Å, which is significantly shorter than those spanned by the organic spacers (13.7−16.3 Å). Although the chain, with a M^{2+}:N_3^-:COO^- ratio of 1:2:1, is formally negatively charged, the 3D framework is positively charged owing to the overcompensation of the chain charge by the interchain cationic pyridinium groups. The positive framework charge is compensated for by the perchlorate anions, which are enclosed within the interchain channels.

Compound 2. This compound contains 2D cationic coordination layers and mononuclear complex anions, and the layer consists of $[Mn(N_3)(COO)_2]_n$ chains connected by dipyridinium spacers. There are two crystallographically independent Mn^{II} ions. The unique metal ion (Mn1) of the layer resides on an inversion center and assumes an axially elongated trans-octahedral $[N_2O_4]$ geometry similar to that for Mn2 and Mn3 in **1**, with four equatorial oxygen atoms (O1, O1E, O2B, and O2D) from different carboxylate groups and two axial nitrogen atoms (N3 and N3H) from azide ions (Figure 2). The neighboring Mn1 ions are triply bridged by two carboxylate groups in the syn−syn mode and an azide ligand in the EO mode, generating an infinite chain of corner-sharing octahedra along the *b* direction (Figure 3a). The $Mn(OCO)_2(N_3)Mn$ moiety has a crystallographic mirror passing the two carboxylate carbon atoms and the three azide nitrogen atoms. Selected structural parameters for the bridging moiety are listed in Table 3. The Mn−N, Mn−N−Mn, and Mn···Mn parameters are comparable to those between Mn1 and Mn3 in **1**. The Mn−O−C−O torsion angles indicate moderate distortions of the carboxylate bridges from the ideal syn−syn mode. The chains in **2** and **1**, both having $(OCO)_2(N_3)$ triple bridges, show evident differences. In **1**, two independent bridging moieties (A and B) with apparently different structural parameters alternate in the AABB sequence, while all of the bridging moieties in **2** are identical. The uniform chain in **2** is linear, which is dictated by the centrosymmetric trans-octahedral geometry for all metal ions, while the alternating chain in **1** assumes a sigmoidal shape, which arises from alternation of the cis- and trans-octahedral geometries along the chain.

The interchain connection in **2** is completely different from that in **1**. The L ligand also acts as a μ_4 bridge via its

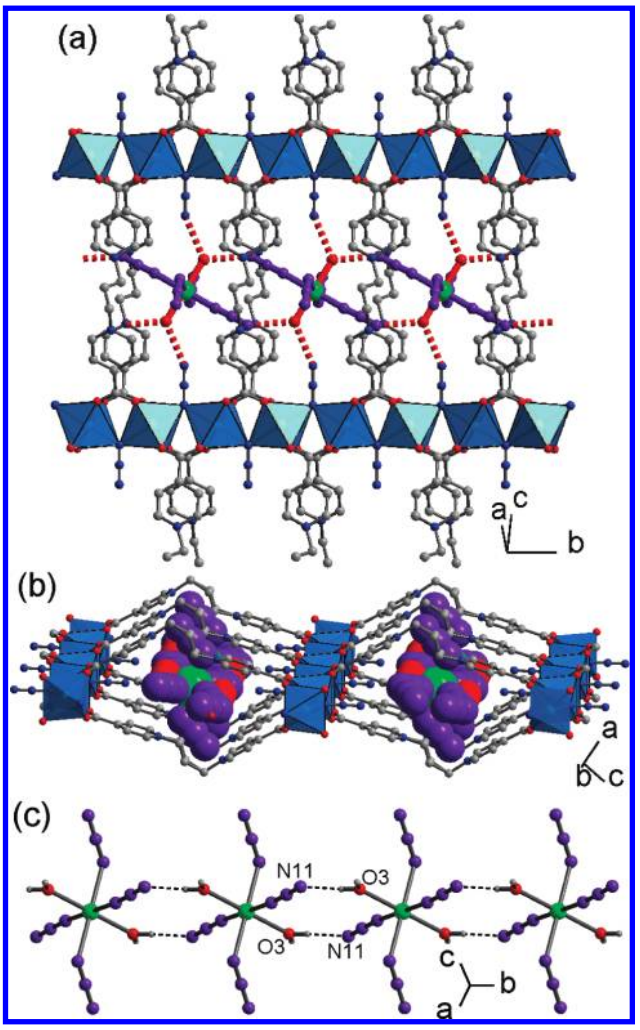

Figure 3. Views showing the structure of **2**: (a) 2D coordination layer based on $Mn(COO)_2(N_3)$ chains and the enclosed hydrogen-bonded chains formed from the mononuclear species; (b) side view of the layer with enclosed hydrogen-bonded chains; (c) hydrogen-bonded chain.

Table 3. Selected Distances (Å) and Angles (deg) for the Bridging Networks in **3**[a]

For $Mn(N_3)_2Mn$			
Mn1−N3(Å)	2.2780(17)	Mn1−N3A	2.2050(17)
Mn1−N3−Mn1A	101.82(7)	Mn1···Mn1A	3.480(1)
For $Mn(OCO)_2Mn$			
Mn1−O1	2.1378(14)	Mn1−O2B	2.1722(14)
Mn1−O1−C1−O2	5.95(31)	Mn1B−O2−C1−O1	89.74(24)
Mn1···Mn1B	4.511(1)	Mn1−O5	2.2836(17)

[a] Symmetry codes: (A) $2-x, 1-y, 1-z$; (B) $1-x, 1-y, 1-z$; (C) $1+x, 1+y, 1+z$.

two carboxylate groups, and the trimethylene tether takes the trans−gauche conformation, which also leads to a bent shape for the whole ligand. The ligands appear in pairs, with each pair binding the same four metal ions from two adjacent chains. Consequently, each chain in **2** is linked to two (instead of four) adjacent chains to generate a 2D layer network extending along the (10−1) plane (Figure 3b). The pairwise bent ligands appear as arch bridges connecting adjacent chains above and below the layer plane. This generates large open channels parallel to the chain, as revealed by a side view of the layer

along the *b* direction. The alternation of the arch bridges on two opposite sides of the chain also leaves large open windows between adjacent chains, as revealed by a view of the layer from above (Figure 3a). The 2D layer is positively charged, in which the anionic chains are overcompensated for in charge by the interchain cationic pyridinium groups.

To compensate for the charge and to avoid emptiness, a hydrogen-bonded chain of mononuclear $[Mn(N_3)_4(H_2O)_2]^{2-}$ anions is enclosed in the open space of the coordination layer of **2**. In the complex anion, the unique metal ion (Mn2) is located at a centrosymmetric $[N_4O_2]$ environment with two equivalent azide ions and two equivalent water molecules at the equatorial plane and two other equivalent azide ions at axial positions (Figure 3b). The axial Mn−N distances [Mn2−N6 = 2.305(7) Å] are longer than the equatorial Mn−N/O distances [Mn2−O3 = 2.180(7) Å and Mn2−N9 = 2.097(10) Å], and the cis O−Mn−N/O angles fall in the narrow range 86.62(13)−93.38(13)°, defining a trans-octahedral geometry with axial elongation. The mononuclear complex ions are associated into chains through strong and quasi-linear O−H···N hydrogen bonding, which involves a water molecule from one complex ion and a terminal azide nitrogen atom from another complex ion, with O3−H3W1···N11 = 176.52(16)°, H3W1···N11 = 1.918(17) Å, and O3···N11 = 2.782(8) Å. As shown in Figure 3c, a 12-membered ring with self-complementary double hydrogen bonds, $[Mn(O-H\cdots N-N-N)_2Mn]$, is formed between neighboring complex ions, with a Mn···Mn separation of 7.623(3) Å (the *b* length of the unit cell). The hydrogen-bonded chains run along the same direction (the crystallographic *b* direction) as the $[Mn(N_3)(COO)_2]_n$ chains and thread through the channels surrounded by the organic "arch bridges" (Figure 3b). The hydrogen-bonded and coordination chains are connected by another set of O−H···N hydrogen bonds, which are formed between the water molecules from the former chain and the terminal nitrogen atoms of the EO-azide bridges in the latter chain. The relevant parameters are O3−H···N5 = 144.4(6)°, H···N5 = 2.1(1) Å, and O3···N5 = 2.84(15) Å. To complete the 3D lattice in **2**, the filled layers are packed in parallel in an offset way, with the small interlayer apertures being occupied by free water molecules (see the Supporting Information).

Compound 3. This compound contains a 2D coordination network in which 1D Mn^{II} chains with alternating double EO-azide and double carboxylate bridges are linked by the organic L ligands. The coordination environments are shown in Figure 4a. The unique Mn^{II} ion in the structure resides in an asymmetric *pseudo*octahedral $[N_2O_4]$ environment, with three carboxylate oxygen atoms (O1, O2B, and O4C) defining a triangular face and two azide nitrogen atoms (N3 and N3A) plus a water oxygen (O5) defining the opposite face. The Mn−N and $Mn-O_{water}$ distances [2.2050(17)−2.2836(17) Å] are somewhat longer than $Mn-O_{carboxylate}$ [2.1378(14)−2.1722(14) Å. The neighboring manganese atoms are alternately doubly bridged by two EO-azide ligands and two carboxylate groups, generating an infinite chain along the *a* direction (Figure 4b). Selected bridging parameters are given in Table 3. The double EO-azide bridging

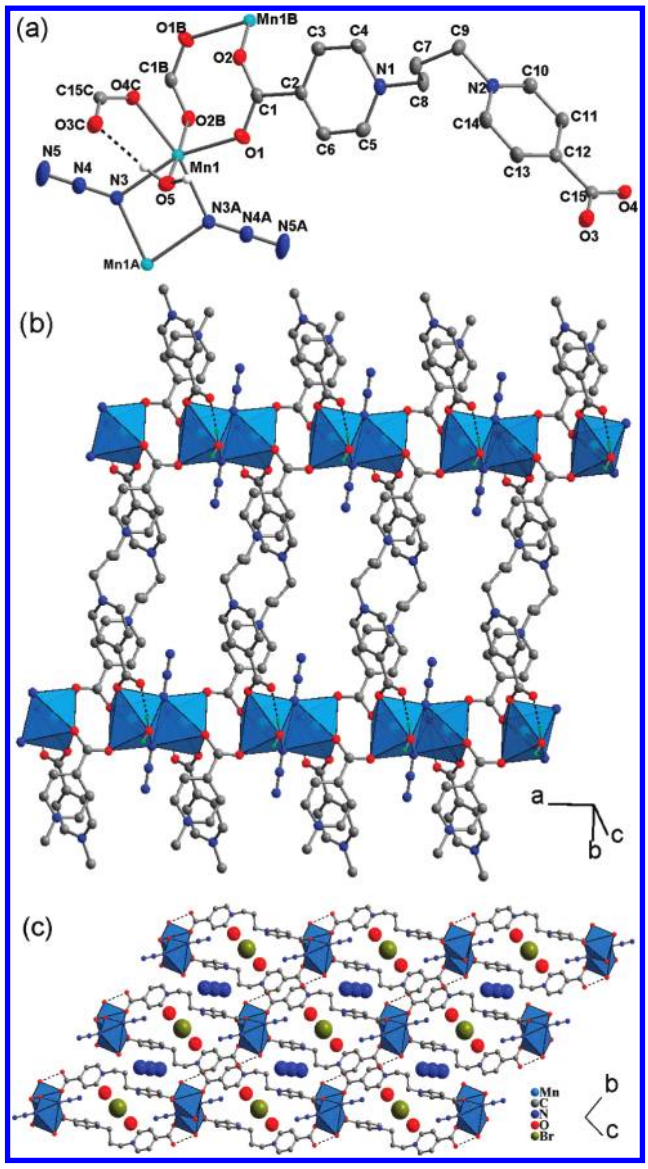

Figure 4. (a) Local coordination environments of the manganese center and the ligands in compound **3**. Hydrogen atoms attached to carbon atoms are omitted for clarity, and symmetry codes are (A) $2-x, 1-y, 1-z$, (B) $1-x, 1-y, 1-z$, and (C) $1+x, 1+y, 1+z$. (b) 2D network formed by the L ligand interlinking the chains with alternating double EO-azide and double carboxylate bridges. (c) View showing the 3D packing of the layers and the lattice azides, bromides, and water molecules.

moiety is centrosymmetric and forms a planar $[Mn_2N_2]$ parallelogram ring; the Mn−N−Mn and Mn···Mn parameters fall within the normal ranges for such bridges.[4a,9,26] The double carboxylate bridging moiety is also centrosymmetric, and the eight-membered $[Mn_2(OCO)_2]$ ring assumes a chairlike conformation. It is noteworthy that the carboxylate bridge adopts an uncommon mode intermediate between syn−syn and syn−anti. For both syn and anti coordination mode, the metal atom usually lies in or near the OCO plane, with the M−O−C−O torsion

(26) (a) Karmakar, T. K.; Ghosh, B. K.; Usman, A.; Fun, H.-K.; Rivière, E.; Mallah, T.; Aromí, G.; Chandra, S. K. *Inorg. Chem.* **2005**, *44*, 2391. (b) Das, A.; Rosair, G. M.; Salah El Fallah, M.; Ribas, J.; Mitra, S. *Inorg. Chem.* **2006**, *45*, 3301. (c) Ni, Z.-H.; Kou, H.-Z.; Zheng, L.; Zhao, Y.-H.; Zhang, L.-F.; Wang, R.-J.; Cui, A.-L.; Sato, O. *Inorg. Chem.* **2005**, *44*, 4728. (d) Liu, B.-L.; Xiao, H.-P.; Nfor, E.-N.; Song, Y.; You, X.-Z. *Inorg. Chem. Commun.* **2009**, *12*, 8.

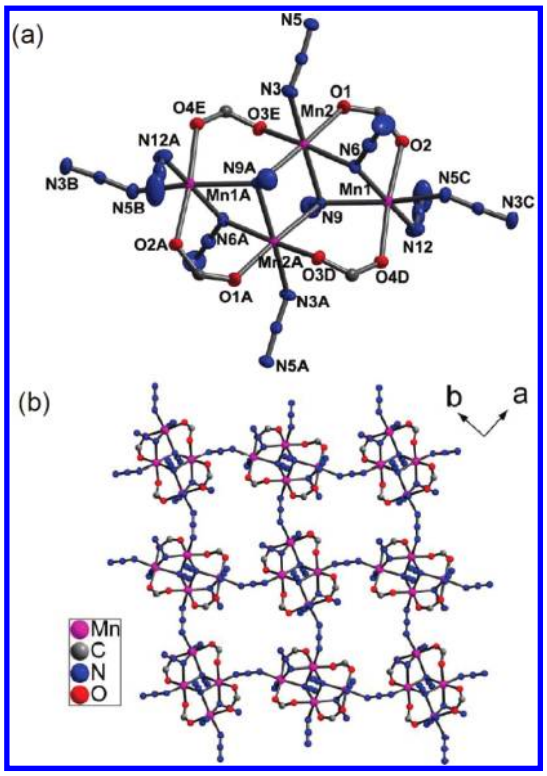

Figure 5. (a) Tetranuclear manganese cluster in compound **4**. Hydrogen atoms are omitted for clarity, and symmetry codes are (A) $-x, -y, 1-z$, (B) $-{}^1/_2-x, -{}^1/_2+y, z$, (C) ${}^1/_2+x, {}^1/_2-y, 1-z$, (D) $1+x, {}^1/_2-y, 0.5+z$, and (E) $-1-x, -{}^1/_2+y, {}^1/_2-z$. (b) (4,4) networks formed by connecting the clusters with azide.

angles being ideally 0 and 180°, respectively. In **3**, the carboxylate bridge has one metal ion nearly in its plane (M−O−C−O ≈ 6°), but the other metal ion deviates significantly from the plane, as indicated by the large M−O−C−O angle of about 90°.

Unlike that in **1** and **2**, the L ligand in **3** serves as a μ_3 bridge, with a bridging carboxylate group binding two metal ions (via O1 and O2) from one chain and a monodentate carboxylate group binding a metal ion (via O4) from another chain. The uncoordinated carboxylate oxygen (O3) forms a hydrogen bond with the coordinated water molecule (Figure 4a), with O5−H5B···O4C = 107.27(18)°, H5B···O3C = 1.884(23) Å, and O3C···O5 = 2.719(3) Å. The overall interchain connection is similar to that in **2**. The chains are connected into a 2D layer network along the (01−1) direction (Figure 4b), in which the bent ligands serve as pairwise archlike bridges above and below the layer plane. The 2D layers are also positively charged and packed in an offset way. The intralayer open space is occupied by free bromide ions and water molecules, while free azide ions are located in the interlayer apertures (Figure 4c).

Compound 4. This compound has been reported in our previous communication.[22a] A brief description of the structure focusing on the bridging network is presented here for the convenience of comparison with other compounds. The compound is based on butterfly-like $[Mn_4(\mu_3\text{-}N_3)_2(\mu_2\text{-}N_3)_2(\mu_2\text{-}COO)_4]$ clusters (Figure 5a), in which the two "body" manganese ions are doubly bridged by two μ_3-EO-azide (or 1,1,1-azide) ligands, while the "body" and "wing-tip" manganese ions are either doubly

Table 4. Selected Distances (Å) and Angles (deg) for the Bridging Networks in **4**[a]

	For $(EO\text{-}N_3)_2$		
Mn2−N9	2.2793(19)	Mn2−N9−Mn2A	92.80(7)
Mn2−N9A	2.2843(18)	Mn2···Mn2A	3.3047(7)
	For $(OCO)(EO\text{-}N_3)_2$		
Mn1−O2	2.2610(16)	Mn1−O2−C15−O1	3.22(39)
Mn2−O1	2.1167(18)	Mn2−O1−C15−O2	0.95(41)
Mn1−N9	2.3435(19)	Mn1−N9−Mn2	92.27(7)
Mn2−N6	2.209(2)	Mn1−N6−Mn2	97.30(8)
Mn1−N6	2.231(2)	Mn1···Mn2	3.3334(5)
	For $(OCO)(EO\text{-}N_3)$		
Mn1−O4D	2.1749(17)	Mn1−O4D−C1D−O3D	8.41(38)
Mn2−O3E	2.1269(18)	Mn2A−O3D−C1D−O4D	60.56(33)
Mn1−N9−Mn2A	116.48(8)	Mn1···Mn2A	3.9350(5)
	For Single $EE\text{-}N_3$		
Mn2−N3	2.196(2)	Mn2−N3−N4	121.98(2)
Mn1C−N5	2.215(2)	Mn1C−N5−N4	134.2(2)
Mn2···Mn1C	5.9150(5)	Mn2−N3−N4−N5−Mn1C	123.66(17)

[a] Symmetry codes: (A) $-x, -y, 1-z$; (B) $-{}^1/_2-x, -{}^1/_2+y, z$; (C) $-{}^1/_2+x, {}^1/_2-y, 1-z$; (D) $1+x, {}^1/_2-y, 0.5+z$; (E) $-1-x, -{}^1/_2+y, {}^1/_2-z$.

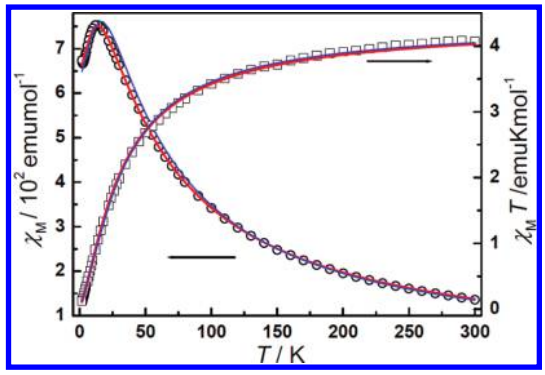

Figure 6. Temperature dependence of χ and χT for **1**. The solid lines represent the fits to Fisher's equation (eq 1) for uniform chains (blue line) and our equation (eq 5) for $J_1J_1J_2J_2$ alternating chains (red line) (see the text).

bridged by a μ_3-EO-azide and a syn−syn carboxylate bridge or triply bridged by a μ_3-EO-azide, a μ_2-EO-azide, and a syn−syn carboxylate bridge. Selected distances and angles for the bridging networks are given in Table 4. Each cluster is connected with four equivalent clusters through four equivalent μ_2-EE-azide bridges, producing a complex layer with mixed azide and carboxylate bridges (Figure 5b). The layers are interlinked by the L ligands to generate a complex 3D framework, which represents an unprecedented self-catenated 3D net (Schläfli symbol $4^{16}\cdot6^{12}$).[22a]

Magnetic Properties. Magnetic measurements were carried out on polycrystalline samples of **1**−**4** under 1000 Oe in the range of 2−300 K, and the χ and χT vs T plots are given in Figures 6−9, respectively. According to the structural data, all of the compounds except **4** contain Mn^{II} chains interlinked by the L ligands. Considering the long interchain Mn···Mn distances, the systems could be treated as magnetically isolated 1D chains.

Complex 1. The χT value per Mn^{II} for this compound at 300 K is about 4.08 emu K mol^{-1}, lower than the spin-only value (4.38 emu K mol^{-1}) expected for a magnetically

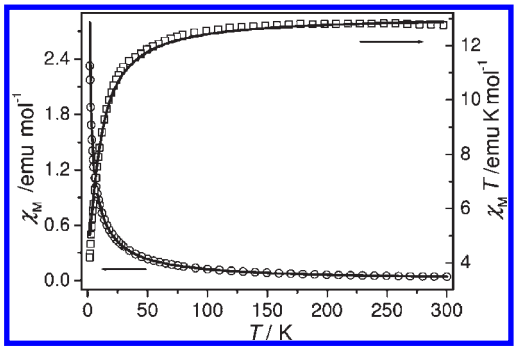

Figure 7. Temperature dependence of χ and χT for **2**. The solid lines represent the fit to the model for uniform chains (see the text).

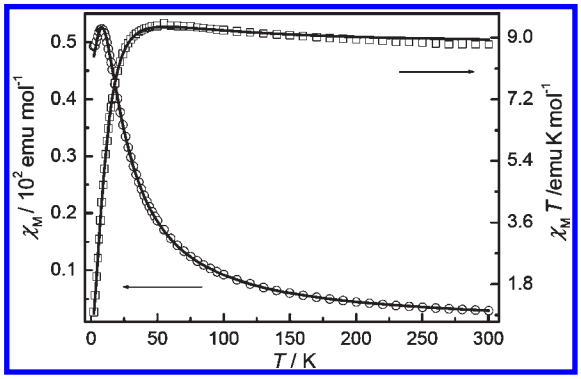

Figure 8. Temperature dependence of χ and χT for **3**. The solid lines represent the fit to the conventional equation for an alternate chain (see the text).

isolated high-spin Mn^{II} ion. As the sample is cooled from room temperature, the χT value decreases continuously, while the χ value increases to a broad maximum at about 14 K and then decreases upon further cooling. The data above 70 K follow the Curie−Weiss law with $C = 4.58$ emu K mol^{-1} and $\theta = -33.9$ K, indicating antiferromagnetic coupling interactions between the neighboring Mn^{II} centers.

Two different classical-spin models have been utilized to simulate the experimental magnetic behavior.

(1) The first model assumes that the system can be treated as a uniform chain in which the magnetic interactions between neighboring metal ions are identical. Then the interaction (J) can be expressed by the spin Hamiltonian $H = -J\sum S_i S_{i+1}$. In the classical-spin approximation, the following expression (eq 1) of magnetic susceptibility was deduced by Fisher.[27]

$$\chi_{chain} = [Ng^2\beta^2 S(S+1)/3kT][(1+u)/(1-u)] \qquad (1)$$

where u is the Langevin function $u = \coth[JS(S+1)/kT] - kT/[JS(S+1)]$, with $S = {}^5/_2$. The best simulation of the experimental data of **1** led to $J = -2.75$ cm^{-1} with g fixed at 2.00. As shown in Figure 6, the agreement between the experimental data and the simulated line (blue) is good above 100 K, but the fit is somewhat unsatisfactory in the low-temperature range, with the maximum of the calculated $\chi-T$ curve deviating toward higher temperature.

(2) Considering that the chain in **1** actually contains two structurally different sets of triple bridges alternating in the AABB sequence, it is best described as a 1D

(27) Fisher, M. E. *Am. J. Phys.* **1964**, *32*, 343.

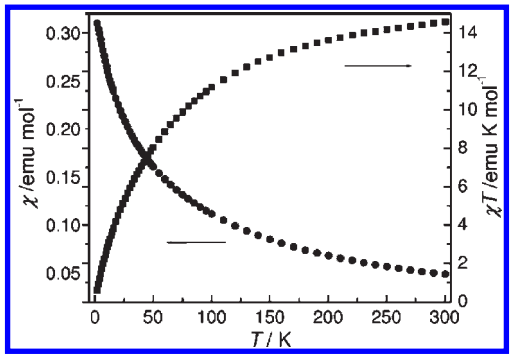

Figure 9. χT and χ vs T plots for **4**.

Chart 2

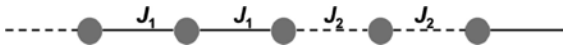

Heisenberg system with alternating $J_1J_1J_2J_2$ interactions (Chart 2). To our knowledge, no analytical expression for such systems is available prior to this study. Following the general methodology applied by Fisher[27] and others[28] for uniform and different alternating chains, a convenient expression in the classical-spin approximation can be deduced. In this case, the spin Hamiltonian can be expressed as

$$H = -J_1\sum_{i=0}(S_{4i+1}S_{4i+2} + S_{4i+2}S_{4i+3}) - J_2\sum_{i=0}(S_{4i+3}S_{4i+4} + S_{4i+4}S_{4i+5}) \qquad (2)$$

Generally, the wave-vector-dependent susceptibility[29] is given by

$$S(q) = \frac{1}{NkT}\sum_{n,p}\langle S_n S_{n+p}\rangle \exp(iqp) \qquad (3)$$

where the pair correlation function between spin operators located at sites n and $n+p$, in our case, can be written as

$$\langle S_n S_{n+p}\rangle = u_1u_1u_2u_2u_1u_1u_2u_2... \qquad (4)$$

where u_1 and u_2 are the Langevin functions corresponding to J_1 and J_2, respectively.

Then, following the general procedure,[21] the expression of the bulk susceptibility per site in the $q = 0$ limit can be deduced as

$$\chi = \frac{N\beta^2g^2}{12kT}S(S+1)\frac{A}{B} \qquad (5)$$

$$A = 4 + 4u_1 + 4u_2 + 4u_1u_2 + 2{u_1}^2 + 2{u_2}^2 + 4{u_1}^2u_2 + 4u_1{u_2}^2 + 4{u_1}^2{u_2}^2$$

$$B = 1 - {u_1}^2{u_2}^2$$

(28) (a) Cano, J.; Journaux, Y.; Goher, M. S. A.; Abu-Youssef, M. A. M.; Mautner, F. A.; Reiâ, G. J.; Escuer, A.; Vicente, R. *New J. Chem.* **2005**, *29*, 306. (b) Abu-Youssef, M. A. M.; Drillon, M.; Escuer, A.; Goher, M. A. S.; Mautner, F. A.; Vicente, R. *Inorg. Chem.* **2000**, *39*, 5022. (c) Cortés, R.; Drillon, M.; Solans, X.; Lezama, L.; Rojo, T. *Inorg. Chem.* **1997**, *36*, 677.

(29) Thorpe, M. F. *J. Phys.* (*Paris*) **1975**, *36*, 1177.

It is noted that this expression reduces exactly to eq 1 when $u_1 = u_2$.

As shown in Figure 6, eq 5 can simulate the experimental data of **1** better than eq 1, especially in the region around the maximum. The best fit led to $J_1 = -4.27\ cm^{-1}$ and $J_2 = -1.19\ cm^{-1}$ with g fixed at 2.00. The J_1 and J_2 values confirm that appreciably different magnetic interactions are mediated through the alternating triple bridges.

The magnetic interaction through mixed bridges should be the cooperative or competitive effect of the different exchange pathways. The syn−syn or syn−anti carboxylate bridge always induces antiferromagnetic coupling between Mn^{II} ions, as has been observed in a number of compounds with single or double carboxylate bridges.[12−16] For the EO-azide bridge, it is believed that the coupling is dependent upon the M−N−M bridging angle. Density function theory calculations[30] on binuclear Mn^{II} systems suggested that the bridge induces ferromagnetic coupling for Mn−N−Mn angles $>98°$, which has been experimentally verified in many systems.[4a,9,26] Magnetic analyses on **1** suggest that the interplay among the two carboxylate and one azide pathways leads to an overall antiferromagnetic coupling, although the Mn−N−Mn angles (111.1° and 117.4°) imply ferromagnetic exchange through the azide pathway. The strength of the overall coupling in such systems could be influenced by a number of factors, including the Mn−N/O distances, the Mn−N−Mn angle, the distortion of the Mn−O−C−O−Mn pathway, and the Mn···Mn distance. According to the structural data of **1** (Table 2), the bridges between Mn1 and Mn2 have shorter Mn−N/O and Mn···Mn distances, a smaller Mn−N−Mn angle, and smaller Mn−O−C−O angles than the bridges between Mn1 and Mn3. We tentatively assign the larger J_1 parameter to the Mn1···Mn2 interaction and J_2 to that for Mn1···Mn3. The assignment is supported by the data obtained for **2** (see below).

Complex 2. The χT value per formula for this compound at 300 K is about 12.76 emu mol^{-1} K, lower than the spin-only value (13.125 emu mol^{-1} K) expected for three magnetic isolated high-spin Mn^{II} ions. As the temperature is lowered, the χT value decreases continuously, while the χ value increases monotonically (Figure 7). The data above 80 K follow the Curie−Weiss law with $C = 4.86$ emu K mol^{-1} and $\theta = -2.0$ K, indicating antiferromagnetic coupling interactions between the neighboring Mn^{II} centers.

The experimental magnetic behavior of **2** has also been simulated by two different approaches.

(1) According to the structural data, the system can be treated as 1D uniform Mn^{II} chains plus mononuclear Mn^{II} species. The magnetic contribution of the chain (χ_{chain}), in which magnetic coupling (J) is mediated through the $(OCO)_2(EO\text{-}N_3)$ triple bridges, can be described by eq 1. Then, according to the stoichiometry of the compound, the total susceptibility is $\chi = 2\chi_{chain} + \chi_{mono}$, where $\chi_{mono} = Ng^2\beta^2S(S+1)/3kT$ is the contribution from the mononuclear component. The simulation leads to $J = -1.02\ cm^{-1}$ with g fixed at 2.00. The J value indicates that weak antiferromagnetic interactions are operative through the triple bridges in **2**.

(2) Considering that the mononuclear complex ions are associated into 1D uniform chains through O−H···N hydrogen bonds, the total susceptibility can be expressed as $\chi = 2\chi_{chain} + \chi'_{chain}$, where χ_{chain} is for the coordination chain as described above and χ'_{chain} for the hydrogen-bonded chain. The expression of χ'_{chain} is obtained from eq 1 by replacing u with u', which corresponds to the interaction (J') mediated through the hydrogen bonds. This approach yielded a slightly better simulation than the first, with the best-fit parameters being $J = -0.92\ cm^{-1}$ and $J' = -0.06\ cm^{-1}$ with g fixed at 2.00. The J value is comparable to that obtained by the first approach, and the J' value indicates very weak antiferromagnetic coupling through the hydrogen bonds.

The antiferromagnetic interaction through the $(OCO)_2(EO\text{-}N_3)$ triple bridge (denoted as B2 for convenience) in **2** is very similar to that (denoted as B13) between Mn1 and Mn3 in **1** but much weaker than that (denoted as B12) between Mn1 and Mn2 in **1**. As can be easily seen from the data listed in Table 2, the Mn−N and Mn−N−Mn parameters for B2 and B13 are almost identical, but these parameters for B12 in **1** are appreciably smaller. This suggests that the Mn−N and Mn−N−Mn parameters are important in determining the magnitude of the interaction. The larger these parameters, the weaker the interaction. This trend is also followed in the only previous Mn^{II} compounds with similar bridges, which exhibits an intermediate interaction of $J = -3.0\ cm^{-1}$.[22b] When compared with B12, the bridge in this previous compound has a similar Mn−N−Mn angle [111.1(1)°] but a significantly longer Mn−N distance [2.259(3) Å], which leads to a decreased interaction. When compared with B2 and B13, it can be assumed that the effect of increasing Mn−N is overtaken by the significant decrease in Mn−N−Mn, so an increased interaction is observed. The carboxylate bridges in the above compounds also show differences in the Mn−O distances and Mn−O−C−O torsion angles, but no unambiguous magnetostructural relationship can be derived.

Complex 3. The χT value per formula for this compound at 300 K is ca. 8.80 emu K mol^{-1}, comparable with the value expected for two magnetically isolated Mn^{II} ions with $g = 2.00$. As the temperature is lowered, the χT value first increases slowly to a rounded maximum of 9.42 emu mol^{-1} K at 55 K and then decreases rapidly, while χ first increases smoothly to reach a maximum of 0.524 emu mol^{-1} at about 8 K and then decreases upon further cooling (Figure 8). The data above 100 K follow the Curie−Weiss law with $C = 8.57(1)$ emu K mol^{-1} and $\theta = 7.90(4)$ K. The above features indicate that competitive antiferro- and ferromagnetic interactions are operative in **3**, and the high-temperature behavior implies that the ferromagnetic interaction is stronger than the antiferromagnetic one.

These are consistent with the presence of two alternating bridges along the chain in **3**, and the system can magnetically be treated as classical-spin chains with alternating J_1J_2 interactions. On the basis of the spin Hamiltonian given in eq 6, the expression of magnetic susceptibility (corresponding to two spin sites)

(30) Ruiz, E.; Cano, J.; Alvarez, S.; Alemany, P. *J. Am. Chem. Soc.* **1998**, *120*, 11122.

for such systems has been deduced by Cortés et al.[28c] as eq 7.

$$H = -J_1 \sum S_{2i+1}S_{2i+2} - J_2 \sum S_{2i+2}S_{2i+3} \quad (6)$$

$$\chi = [Ng^2\beta^2 S(S+1)/3kT][(1+u_1+u_2+u_1u_2)/(1-u_1u_2)] \quad (7)$$

Here u_1 and u_2 are the Langevin functions corresponding to J_1 and J_2, respectively, as defined above in eq 1 ($S = {}^5/_2$). With the g parameter fixed at 2.0, the best fit of the experimental data led to $J_1 = 3.15$ cm^{-1} and $J_2 = -1.54$ cm^{-1}. The results confirm alternating ferro- and antiferromagnetic interactions. The J_1 value for the ferromagnetic interaction falls within the usual range of 1−10 cm^{-1} for double EO-azide bridges between Mn^{II} ions,[4a,9,26] while the J_2 value for the weak antiferromagnetic interaction falls within the range of −2 to 0 cm^{-1} for similar double carboxylate bridges observed in a few Mn^{II} compounds.[13a,14−16]

Complex 4. The χT value per Mn_4 unit for this compound is 14.58 emu mol^{-1} K at 300 K, significantly lower than the spin-only value (17.5 emu mol^{-1} K) for four isolated Mn^{II} ions. Upon cooling, χ and χT exhibit monotonic increases and decreases, respectively (Figure 9). The data above 15 K follow the Curie−Weiss law, with $\theta = -57.8$ K and $C = 17.48$ emu mol^{-1} K. The large negative θ value suggests an overall antiferromagnetic behavior.

Magnetically, **4** can be regarded as Mn_4 cluster-based layers with four different sets of short bridging systems between metal ions, including three intracluster sets [(EO-N_3)$_2$, (OCO)(EO-N_3)$_2$, and (OCO)(EO-N_3)] and one intercluster set (single EE-N_3). Four different interaction parameters are needed to describe the magnetic behavior, and it is unwarranted to neglect any of them. Because of the lack of an appropriate model for such a system, we cannot quantitatively evaluate these parameters. However, we give a tentative and qualitative analysis on the nature of the interactions based on the known magnetostructural information for related systems.

Let us begin with the double EO-azide bridge between the two "body" metal ions (Mn2 and Mn2A; Figure 5a). Double EO-azide bridges usually have Mn−N−Mn = 99−105° and induce ferromagnetic coupling, as demonstrated in **3** and a number of previous compounds.[4a,9,26] However, theoretical studies suggest a crossover from ferro- to antiferromagnetic when Mn−N−Mn is smaller than the critical angle 98°.[30] In **4**, the bridge has Mn−N−Mn = 92.8°, significantly smaller than the critical angle, so it may be assumed to propagate antiferromagnetic coupling. This is open to discussion based on further experimental systems with similar angles.

There are two different types of magnetic interactions between the "body" and "wing-tip" Mn ions in the cluster, corresponding to the (OCO)(EO-N_3)$_2$ and (OCO)(EO-N_3) bridges. Because of the complexity arising from the mixing of the different bridges (such as complementarity and anticomplementarity[1b]) and from the large number of singly occupied orbitals involved in Mn^{II}, it is difficult to deduce the magnetostructural information for such systems. However, we note that all of the known Mn^{II} complexes with simultaneous azide and carboxylate bridges exhibit antiferromagnetic interactions, whether the bridges are double or triple. The (OCO)(EO-N_3) double bridges have been observed in a few Mn^{II} compounds,[19a,b] with Mn−N−Mn being about 120° and interaction parameters in the range of −1.5 to +2.5 cm^{-1}. Two Mn^{II} complexes with (OCO)(EO-N_3)$_2$ triple bridges have recently been reported by us,[22c] which have Mn−N−Mn ≈ 94° and $J \approx -5$ cm^{-1}. In **4**, the double and triple bridges are similar to those in the previous compounds, with Mn−N−Mn being 116.5° and 94.8°, respectively. Therefore, we could anticipate that intracluster interactions between the "body" and "wing-tip" Mn ions are all antiferromagnetic in nature.

Finally, the "body" and "wing-tip" Mn ions from different clusters should also be antiferromagnetically coupled through single EE-azide bridges. The EE bridge is very common in metal azide compounds, and it always induces antiferromagnetic interactions in the known Mn^{II} compounds.[4a,9a,9b,31]

Conclusion

We have described four different Mn^{II} coordination polymers with azide and dicarboxylate ligands bearing the dipyridiniumpropane spacer. In these compounds, Mn^{II} ions are connected by the azide and carboxylate bridges mixed in different fashions to give different anionic manganese−azide−carboxylate chains (**1**−**3**) or layers (**4**), which are interlinked by cationic organic spacers to 2D (**2** and **3**) or 3D (**1** and **4**) networks. The chain in **1** contains different (OCO)$_2$(EO-N_3) triple bridges alternating in the AABB sequence, while **2** contains identical (OCO)$_2$(N_3) triple bridges. The (OCO)$_2$(EO-N_3) triple bridges induce antiferromagnetic coupling between Mn^{II} ions, and the magnitude of the coupling may be correlated to the Mn−N and Mn−N−Mn parameters. The chain in **3** contains alternating double EO-azide and double carboxylate bridges that induce ferro- and antiferromagnetic interactions, respectively. The layer in **4**, which shows overall antiferromagnetic characteristics, contains unique [Mn_4(μ_3-EO-N_3)$_2$(μ_2-EO-N_3)$_2$(μ_2-OCO)$_4$] clusters interlinked through single μ_2-EE-azide bridges. With this work, we further demonstrated that the incorporation of zwitterionic dicarboxylate ligands into metal azide systems is an efficient approach toward magnetic systems with mixed azide and carboxylate bridges and that the systems exhibit great structural diversity depending upon the synthetic conditions. In addition, the large diversity of the zwitterionic carboxylate ligands offers us great opportunities to systematically investigate the mixed bridging systems for the purpose of unveiling the magnetostructural correlations and constructing new magnetic materials.

Acknowledgment. We are thankful for financial support from NSFC (Grants 20571026 and 20771038) and the Shanghai Leading Academic Discipline Project (B409).

Supporting Information Available: X-ray crystallographic information for compounds **1**−**4** in CIF format, PXRD patterns and IR spectra for compounds **1**−**4**, and supplementary structural graphics for compound **2**. This material is available free of charge via the Internet at http://pubs.acs.org.

(31) (a) Bitschnau, B.; Egger, A.; Escuer, A.; Mautner, F. A.; Sodin, B.; Vicente, R. *Inorg. Chem.* **2006**, *45*, 868. (b) Abu-Youssef, M. A. M.; Escuer, A.; Vicente, R.; Mautner, F. A.; Öhrstrom, L.; Goher, M. A. S. *Polyhedron* **2005**, *24*, 557. (c) Abu-Youssef, M. A. M.; Escuer, A.; Gatteschi, D.; Goher, M. A. S.; Mautner, F. A.; Vicente, R. *Inorg. Chem.* **1999**, *38*, 5716.